A New Class of Frequency Selective Surfaces Based on the Concept of Meta-Materials

Kamal Sarabandi [1] **and Nader Behdad** [2]

[1] *Department of Electrical Engineering and Computer Science, University of Michigan, Ann Arbor, MI, 48109-2122, USA, Tel: (734) 936-1575, Fax: (734) 647-2106, email: saraband@eecs.umich.edu*

[2] *Same as [1] above, email: behdad@engin.umich.edu*

INTRODUCTION

The demand for high performance RF front-end components and devices is on the rise for their vast applications in telecommunications and radar. Frequency selective surfaces as superstrate and magnetic materials and reactive surfaces as substrates for antennas are sought for in order to reduce the antenna's RCS, protecting receiver from jammers and interferers, as well as miniaturizing radiating elements [1]-[2]. The concept of meta-material, artificial materials having constitutive behavior not observed naturally has opened new doors for accomplishing certain functionalities not possible before. These include artificial magnetism, negative permeability or permittivity material with bandgap characteristics, double negative materials, and reactive impedance surfaces (RIS). In recent years it has been shown that by using such materials small antennas with enhanced radiation characteristics, planar lenses, electrically small EM insulators, thin absorbers, etc. can be easily designed and fabricated.

In this paper, we propose a new type of engineered material that can act as a frequency selective surface with any desired order or a reactive impedance surface. The material consists of a periodic array of small metallic patches printed on one side of a dielectric substrate and a wire grid structure printed on the other side, both having the same period. The periodicity of the printed patterns is much smaller than the wavelength of operating frequency. A unit cell of this structure consists of two halves of two adjacent patches backed by a piece of wire on the other side of the substrate. The wire acts as an inductor and the two patches separated by a small gap act as two plates of a printed capacitor. The combination therefore acts as a parallel LC circuit having a band-pass characteristic. The substrate is formed by periodically repeating this unit cell in two dimensions. FSS of any order can be formed by cascading a number of such layers. By choosing the number of layers, controlling the coupling coefficient between layers, and choosing an appropriate resonant frequency of each layer, multi-band and wideband FSS operation can easily be achieved.

REACTIVE IMPEDANCE SURFACE DESIGN

The topology of the RIS is shown in Fig. 1a. It is composed of a periodic array of metallic patches etched on one side of a dielectric substrate and a wire grid printed on the other side of the same substrate. The square metallic patches are periodic in two dimensions (x and y) with equal periods of $D_x=D_y=D<<\lambda$ and have side lengths of D-s, where s is the separation between the two adjacent patches. The wire grid consists of parallel metallic strips with the width of w and has the same period, D, in both directions. The side view of the structure along with one of its constituent unit cells are shown in Fig. 1b. If a y polarized plane wave (i.e., a plane wave with electric and magnetic field components of E_y and H_x, respectively) normally impinges upon the unit cell shown in Fig. 1b, positive and negative charge densities establish along the adjacent edges of the bottom and top patches, respectively. This means that the adjacent edges of the two patches act as the two plates off a capacitor. On the other hand, the wire strip printed on the other side of the dielectric substrate acts as an inductor. The equivalent circuit model of the unit cell, shown in Fig. 2, consists of an inductor and a capacitor separated by a transmission line with length l_1 and impedance Z_1, which represents the dielectric substrate separating the wire grid from the patch array. The free space on both sides of the RIS is modeled by transmission lines with impedances equal to Z_0=377 Ω. l_1 is usually very small compared to a wavelength and hence, the circuit of Fig. 2 acts as a one-pole band-pass filter.

The interaction of a normally incident plane wave with the FSS shown Fig. 1 can be modeled numerically as shown in Fig. 3. In this case one of the constituting unit cells of the FSS is placed in a waveguide with a square cross section. The top and bottom walls of the waveguide are perfect electric conductors (PEC) and its side walls are perfect magnetic conductors (PMC) and hence, the waveguide can support a TEM plane wave. A y polarized plane wave propagating in the negative z-direction impinges upon the structure and the FDTD method is used to compute the transmission and reflection coefficients of the structure (or equivalently the reflection and transmission coefficients from the infinitely

large RIS). Assuming that ℓ_1 is very small, the loaded quality factor of the resonator can be approximated by $Q_L = Z_0\sqrt{C/L}$, where C and L are the equivalent capacitance and inductance of the unit cell. Even though the non zero value of ℓ_1 causes the loaded Q of the unit-cell to be different, the FSS bandwidth can roughly be considered to be inversely proportional to the loaded Q. Fig. 4a shows the reflection and transmission coefficients of FSS for D=5mm, w=1.0 mm and s=0.5 mm and Fig. 4b shows the reflection and transmission coefficients of the FSS for D=5mm, w=2.0 mm and s=0.3 mm. As is observed from these figures, the FDTD results are very well matched to those of the equivalent circuit model. The equivalent circuit model and the physical parameters for the two different unit-cells are presented in Table 1. The inductance value can be changed by controlling the strip widths in the wire grid, w, and the capacitance value can be controlled by changing the separation between the two adjacent metallic patches, s. Increasing C increases the loaded Q and, as seen from Fig. 4b, decreases the bandwidth of the FSS. As can be observed from Fig. 4, the one-pole FSS exhibits a non-zero insertion loss at its center frequency. This is caused by the presence of the thin dielectric substrate between the inductor and capacitor. Furthermore, the insertion loss increases as Q_L increases and this makes the one-pole FSS element a less attractive option for narrow-band applications.

Table 1. Physical and equivalent circuit parameters of two different FSS types.

	w	s	ℓ_1	ε_R	L	C
Type 1	1.0 mm	0.5 mm	0.5 mm	3.4	0.85 nH	0.145 pF
Type 2	2.0 mm	0.3 mm	0.5 mm	3.4	0.37 nH	0.207 pF

In order to circumvent this problem and achieve a sharper band pass behavior, two identical one-pole FSS elements can be cascaded to form a two-pole FSS. The equivalent circuit of such a two-pole FSS is shown in Fig. 5, where it is assumed that the two elements are separated by a distance of l_2 and the space between the two elements is filled with a material with dielectric constant of ε_{R2}. Here ε_{R2} is chosen to be equal to 1 and the separation distance is chosen so that the electrical distance between the two elements is equal to 90° at the center frequency of the pass band. This ensures a maximally flat response in the pass-band. It is also possible to synthesize a different two-pole response, such as Chebychev or elliptical response, by choosing the individual resonators to be different from one another and selecting a different value of l_2. Fig. 6a shows the reflection and transmission coefficients of a two-pole FSS that consists of two type-1 FSSs separated by a distance of 6.5 mm. An excellent agreement between the FDTD simulations and circuit model and a 0 dB insertion loss are observed. Fig. 6b shows a similar result obtained for a two-pole FSS utilizing two identical type-2 FSSs. Since the type-2 FSS has a higher loaded Q, its two-pole version has a much smaller bandwidth. The 3dB bandwidth (in the pass band) of the two-pole type1 FSS is 15.8% whereas the two-pole type2 FSS shows a 3dB bandwidth of only 4.5%. It is also possible to reduce this bandwidth further by increasing the loaded Q of its constituting one-pole FSS, which can be accomplished by increasing C and decreasing L such that the resonant frequency is maintained.

EXPERIMENTAL VERIFICATION

The band-pass behavior of the FSS structure of the previous section can be experimentally verified by fabricating a relatively large piece of it and measuring its reflection and transmission coefficients for a TEM incident wave. In practice, however, this requires having antennas that are able to transmit and receive TEM waves, such as hard horn antennas, at the desired frequency of operation. On the other hand, if the FSS is to be placed in the far field of an ordinary antenna (such that the transmitted wave is close to TEM) its dimensions should be very large so that the effects of diffraction from the edge of the structure are minimized. In the absence of an appropriate set of antennas and as a result of the errors that are associated with the second method, we have used another method to experimentally verify the accuracy of our simulations and predictions of the previous section. Specifically, the FSS structure is placed inside a waveguide and its frequency response is measured. The advantage of this technique is that the waveguide presents a controlled environment which can be simulated with great accuracy. Therefore, two identical FSS sections are placed 6.3 mm apart inside a WR-90 waveguide with inner dimensions of 0.9"×0.4" (22.86 mm × 10.16 mm). Fig. 7 shows the section of the FSS structure that is use inside the waveguide. The sections are fabricated on a 0.5mm thick RO4003 substrate (Rogers Corp.) with dielectric constant of ε_R=3.4. Each section performs as a one-pole waveguide filter with a similar equivalent circuit model as shown in Fig. 2. In this case, it is imperative to note that the Z_0 and Z_1 should be replaced with the Z_{0TE10} and Z_{1TE10}, where Z_{0TE10} and Z_{1TE10} are the TE_{10} mode impedances of the waveguide filled air and the dielectric, respectively. Unlike the TEM waveguides used in the simulation of the infinite FSS, the WR-90 waveguide does not support a TEM wave and the measurement results do not present the response of the two-pole FSS to a normally incident TEM wave but rather they represent the frequency response of a two-pole waveguide filter whose

building blocks are the same as the FSS structure of Fig. 1. Nevertheless, achieving a good match between the predicted and measured results in this experiment can be used to verify the validity of the design and the accuracy of the FDTD simulations used in the previous section.

The frequency response of this two-pole waveguide filter is simulated using the FDTD method and the response is measured using an HP8720D vector network analyzer. The measured and simulated results are presented Fig. 8 where a very good agreement between the two is observed. The measurement results indicate that the two-pole waveguide filter has an insertion loss of 0.2 dB. This loss can mostly be attributed to lack of perfect connection between metallic parts of the FSS sections and the waveguide and also to the dielectric losses. As can be observed from Fig. 8, there is a very good agreement between the simulation and measurement results. The minor discrepancies between the two results can mostly be attributed to errors occurred during the assembly of the two-pole waveguide filter. One example of such errors is the inevitable deviation of the distance between the two resonators from the desired value of 6.3 mm. Nevertheless, this experiment conclusively verifies the accuracy of our simulations and predictions about the operation of FSS of the previous section. After establishing the validity of the simulation results, two identical FSSs with unit-cell dimensions of D=5 mm, s= 1 mm, and w=0.4 mm were fabricated on two 20 cm × 20 cm panels. The responses of the FSSs in the one- and two-pole modes of operation are then measured by using two X-band standard horn antennas. Details of the measurement setup and the measured results will be presented in the symposium.

CONCLUSIONS

A new meta-material based frequency selective surface is introduced. The FSS is equivalent to a band-pass one pole parallel LC filter and multiple sections of such a structure can be cascaded to achieve a higher order band-pass response. It is also shown that the same element can be used to design waveguide filters of arbitrary order. In particular a two-pole waveguide filter was presented.

REFERENCES

[1] B. A. Munk, "Frequency Selective Surfaces: Theory and Design", Wiley Interscience, 1st ed., New York.

[2] H. Mosallaei and K. Sarabandi, "Antenna miniaturization and bandwidth enhancement using a reactive impedance substrate", IEEE. Trans. Ant. and Prop., Vol. 52, pp. 2403-2414, September 2004.

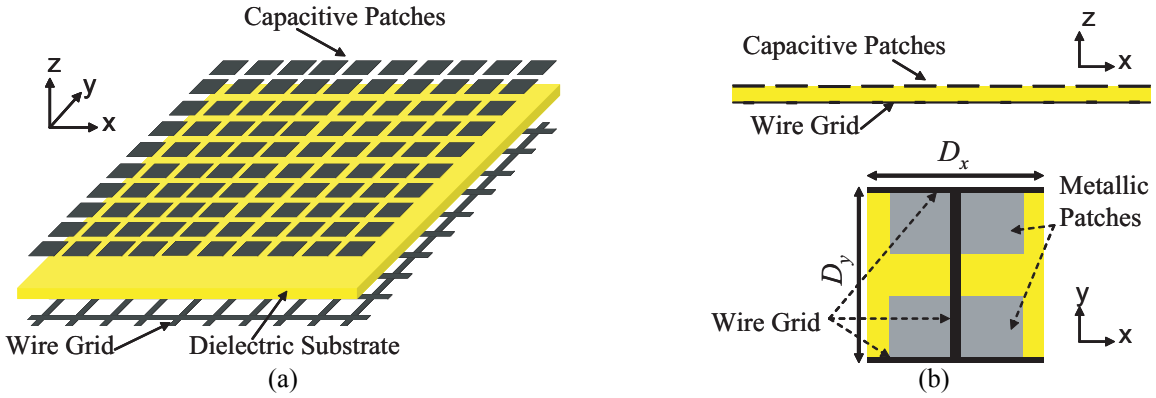

Fig. 1. (a) Three dimensional topology of the one-pole FSS layer. (b) One unit cell of the structure

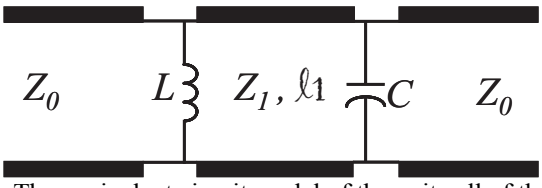

Fig. 2. The equivalent circuit model of the unit cell of the FSS shown in Fig. 1b.

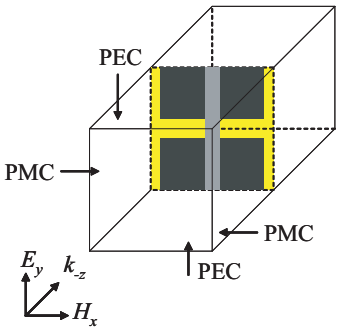

Fig. 3. Unit-cell of the FSS is placed in a TEM waveguide.

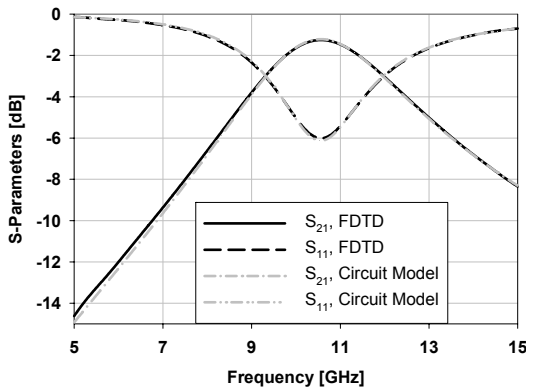

Fig. 4a. Reflection and transmission coefficients for a normally incident TEM wave from the FSS with D=5mm, s=0.5 mm, and w=1 mm.

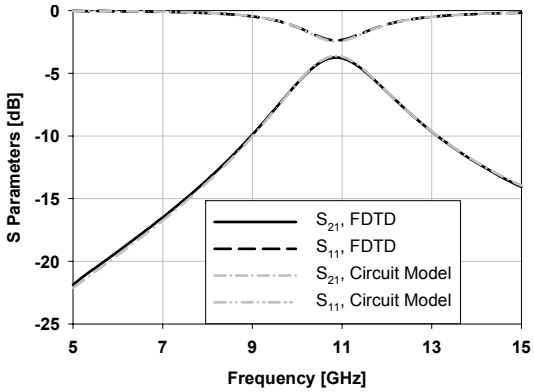

Fig. 4b. Reflection and transmission coefficients for a normally incident TEM wave from the FSS with D=5mm, s=0.3 mm, and w=2 mm.

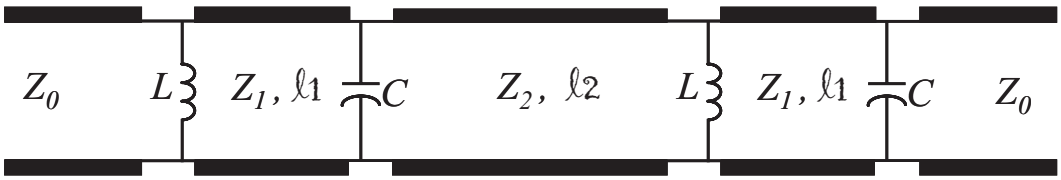

Fig. 5. Circuit model of a two pole FSS utilizing the one-pole FSS shown in Fig. 1a and 1b.

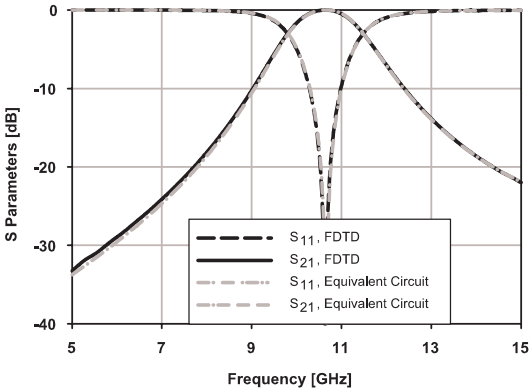

Fig. 6a. Reflection and transmission coefficients for a normally incident TEM wave from the FSS with D=5mm, s=0.5 mm, and w=1 mm.

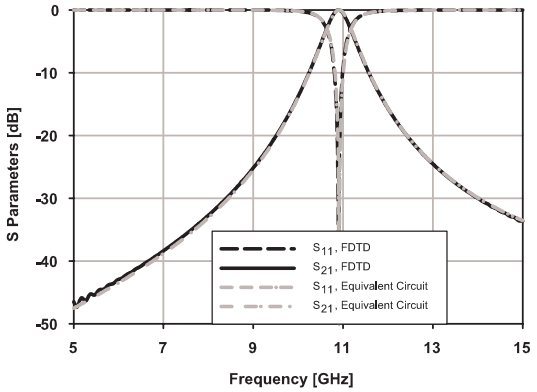

Fig. 6b. Reflection and transmission coefficients for a normally incident TEM wave from the FSS with D=5mm, s=0.3 mm, and w=2 mm.

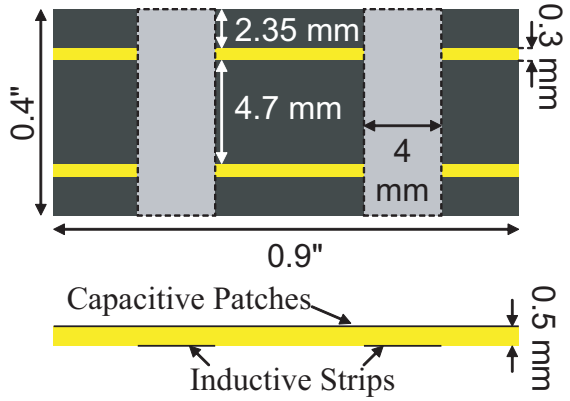

Fig. 7. The one-pole waveguide filter based on two unit-cells of the FSS shown in Fig. 1.

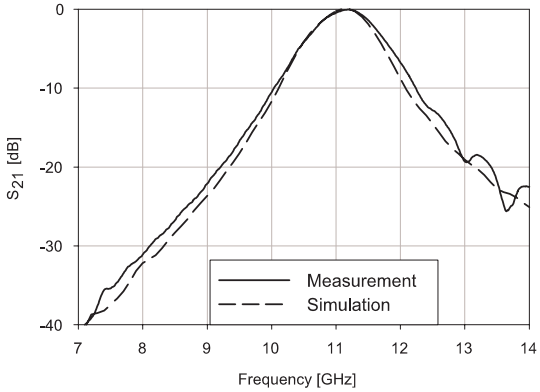

Fig. 8. Measured and simulated transmission coefficients of the two-pole waveguide filter, the constituting blocks of which are shown in Fig. 7.